Evidence for Bilayer Assembly of Cationic Surfactants on the Surface of Gold Nanorods

ARTICLE *in* LANGMUIR · SEPTEMBER 2001

Impact Factor: 4.46 · DOI: 10.1021/la010530o

2 AUTHORS:

Babak Nikoobakht
National Institute of Standards and Technolo…
42 PUBLICATIONS **4,485** CITATIONS
SEE PROFILE

Mostafa A El-Sayed
Georgia Institute of Technology
676 PUBLICATIONS **55,404** CITATIONS
SEE PROFILE

Evidence for Bilayer Assembly of Cationic Surfactants on the Surface of Gold Nanorods

Babak Nikoobakht and Mostafa A. El-Sayed*

School of Chemistry and Biochemistry, Georgia Institute of Technology, Atlanta, Georgia 30332-0400

Received April 9, 2001. In Final Form: July 16, 2001

The surface structure of gold nanorods (NRs) capped with cationic surfactants in water was studied by FTIR, thermogravimetric analysis (TGA), and transmission electron microscopy (TEM). For gold nanorods, the FTIR results show the formation of new bands, which indicate binding of the surfactant headgroup to the surface of the NR. These bands are stable at temperatures as high as 350 °C. For a surfactant mixture (used as capping material), TGA shows a weak weight loss peak at 235 °C and a strong peak at 298 °C assigned to the surfactant molecules in monomer and aggregated forms, respectively. For gold nanorods, three weight loss peaks at about 230, 273, and 344 °C are observed. For gold nanospheres (NSs), TGA shows a strong mass loss at 225 °C and two weak mass loss peaks at 255 and 288 °C. The released material after combustion in the TGA process was analyzed by FTIR spectroscopy and found to be CO_2. Our results suggest the following for both NRs and NSs: (1) There are two different binding modes for the surfactant molecules capping these nanoparticles. (2) Surfactant molecules form a bilayer structure around the gold nanoparticles in which the inner layer is bound to the gold surface via the surfactant headgroups. (3) With increase of the temperature, the outer layer desorbs at lower temperature and consequently the inner layer leaves the surface at higher temperature. (4) The higher desorption temperature of the bilayer in the NRs compared to NSs is explained in terms of the difference in packing of the surfactant molecules and their adsorption energy to the different facets present in these nanoparticles. (5) TEM results suggest that the shape transformation of NRs to NSs occurs as the inner layer is released from the surface. (6) The CH_2 rocking mode at 720 cm^{-1} suggests that the methylene chains have free rotation and surfactants are packed in a hexagonal structure.

Introduction

Assemblies of surfactants or synthetic amphiphiles have been studied as model systems for the understanding of complex natural membranes.[1] In addition, employing synthetic or natural membrane components in surface chemistry and new technologies provide further motivation for understanding and development of these systems.[2]

Some of the surfactants have been utilized as surface stabilizers and/or templates in the synthesis of nanoparticles (NPs). These moieties, by their binding to the nanoparticle surface, decrease the surface energy, control the growth and shape of the particles,[3,4] and act as a stabilizer against coagulation. The presence of a large fraction of atoms on the surface of NPs causes new and/or improved properties and also makes them important in catalysis,[5] chemical sensors, and optoelectronics.[6,7] Metal colloids have also been studied extensively as spectroscopic enhancers.[8]

Neutral surfactants such as alkanethiols,[9] alkylphosphines,[5] and amines[10] are used as stabilizers in the synthesis of different nanoparticles. Charged surfactants have also been used as stabilizers and templates for the growth of a variety of semiconductor and/or metallic nanodots.[11,12] Mixtures of cationic surfactants have recently been utilized as templates to prepare rod-shaped metallic[13] and semiconductor[14] nanoparticles. The mixture consists of cetyltrimethylammonium bromide (CTAB) as the major component and tetraoctylammonium bromide (TOAB) as the minor component.

An important challenge in the area of nanoscale materials is the ability to characterize the structure of the capping agents on the surface of NPs. Techniques such as NMR,[15] Raman,[16] and X-ray photon spectroscopy[17] have been used to study the structure and organization of different capping materials on the surface of NPs. Several studies concerning the adsorption of CTAB on a variety of surfaces have been carried out, though the molecular assemblies of CTAB on hydrophilic surfaces are not fully understood.[18−20] One limitation of the previously studied surfaces has been the small surface area of the substrate,

(1) Fendler, H. J. *Membrane mimetic chemistry*; Wiley: New York, 1982.
(2) Ulman, A. *Chem. Rev.* **1996**, *96*, 1533.
(3) Whetten, R. L.; Gelbart, W. M. *J. Phys. Chem.* **1994**, *98*, 3544.
(4) Leff, D. V.; Ohara, P. C.; Heath, J. R.; Gelbart, W. M. *J. Phys. Chem.* **1995**, *99*, 7036.
(5) Schmid, G., Ed. *Clusters and Colloids*, VCH: Weinheim, 1994.
(6) Weller, H. *Angew. Chem., Int. Ed. Engl.* **1996**, *35*, 1079.
(7) Mirkin, C. A.; Lestinger, R. L.; Mucic, R. C.; Storhoff, J. J. *Nature* **1996**, *382*, 607.
(8) Freeman, R. G.; Grabar, K. C.; Allison, K. J.; Bright, R. M.; Davis, J. A.; Guthrie, A. P.; Hommer. M. B.; Jackson, M. A.; Smith, P. C.; Walter, D. G.; Natan, M. J. *Science* **1995**, *267*, 1629.
(9) Brust, M.; Walker, M.; Bethell, D.; Schiffrin, D. J.; Whyman, R. J. *Chem. Soc., Chem. Commun.* **1994**, 801.
(10) Leif. O.; Brown, L. O.; Hutchison, J. E. *J. Am. Chem. Soc.* **1999**, *121*, 882.
(11) Youn, H. C.; Baral, S.; Fendler, J. H. *J. Phys. Chem.* **1988**, *92*, 6320.
(12) Tanori, J.; Pileni, M. P. *Langmuir* **1997**, *13*, 639.
(13) Ying, Y.; Chang, S. S.; Lee, C. L.; Wang, C. R. C. *J. Phys. Chem. B* **1997**, *101*, 6661.
(14) Chen, C. C.; Chao, C. Y.; Lang, Z. H. *Chem. Mater.* **2000**, *12*, 1516.
(15) a) Becerra, L. R.; Murray, C. B.; Griffin, R. G.; Bawendi, M. G. *J. Chem. Phys.* **1994**, *100* (4) 3297.
(16) Kamogava, K.; Tajima, K.; Hayakawa, K, Kitagawa, T. *J. Phys. Chem.* **1984**, *88*, 2494.
(17) Katari, J. E. B.; Colvin V. L.; Alivisatos, A. P. *J. Phys. Chem.* **1994**, *98* (15) 4109.
(18) Rennie, A. R.; Lee, E. M.; Simister, E. A.; Thomas, R. K. *Langmuir* **1990**, *6*, 1031.
(19) Kung, K.-H. S.; Hayes, K. F. *Langmuir* **1993**, *9*, 263.
(20) Hind, A. R.; Bhargava, S. K.; Grocott, S. C. *Langmuir* **1997**, *13*, 3483.

10.1021/la010530o CCC: $20.00
Published on Web 09/08/2001

which is exposed to the surfactant. However, taking advantage of high surface area of the nanoparticles, it is possible to study the assemblies of surfactants on these active surfaces.

Gold spherical NPs on different substrates as roughening agents have been used in surface-enhanced Raman scattering (SERS).[21] Also the sensitivity of the surface plasmon absorption of these particles toward the dielectric properties of medium has recently been used in developing chemical sensors.[22] A much stronger and more sensitive surface plasmon band for gold nanorods (NRs) compared to spherical particles[13,23] and the ability to form two-dimensional (2D) assemblies[24] make gold NRs suitable substrates in SERS and sensor applications. Therefore knowledge about surface structure of gold NRs is appropriate.

In the present study, FTIR and thermogravimetric analysis (TGA) have been utilized to characterize the structure of the surfactant-capped gold NRs. Transmission electron microscopy (TEM) is also used to monitor the effect of heat on the surface of the gold NRs in conjunction with the above techniques. We raised questions such as: do the surfactants form a micellar or bilayer structure around the NRs? What is the nature of the binding site and how are the surfactants on the surface of gold NRs packed? Finding answers to these questions is also important in helping to understand the role that surfactant plays in the growth mechanism of nanorods.

Experimental Section

Synthesis of Gold Nanorods and Nanospheres. Gold nanorods were synthesized by an electrochemical method,[13] in which a gold electrode is used as the sacrificial anode and a platinum electrode as the cathode. The electrolyte consists of a mixture of cetyltrimethylammonium bromide (CTAB) as a cationic surfactant and tetraoctylammonium bromide (TOAB) as a cosurfactant. The latter surfactant, which has less than 10% contribution in the mixture, induces the cylindrical shape of the gold nanoparticle and the ratio of the two surfactants roughly determines the aspect ratio (the ratio of length to width) of the nanorod. The electrolysis is carried out under continuous ultrasonication and an applied current of 3−5mA for 45 min. Gold nanospheres (NSs) are synthesized using the above procedure either by removing the cosurfactant or by increasing the mole ratio of the surfactant/cosurfactant above 6. The average size of NSs is about 12 nm.

FTIR Spectroscopic Measurements. For mixture of surfactants, a portion of the clear solution (sonicated for 3 h) was deposited on an AgBr window and after air-drying the FTIR spectra were collected. For NRs, a prepared solution was centrifuged twice at 14 000 rpm and 25 °C for 20 min to remove the free surfactant from the solution as much as possible. Depositing the heavily concentrated solution of NRs on AgBr window produced a film of NRs. After air-drying, the sample was kept in a dissicator until the FTIR measurements were made. In the temperature-dependent studies, a thermostat was used for temperatures ranging from 20 to 110 °C and a tube furnace was used for temperatures above 110 °C. Above 110 °C, the data were collected after the sample temperature reached room temperature. Infrared spectra were acquired by using a Nicolet system, Magna model 860. The spectral resolution was 4 cm^{-1} for all the collected data.

TGA Measurements. For the TGA experiments, the highly concentrated solution of gold NRs or NSs was transferred to a platinum crucible. For the surfactant mixture, an ultrasonicated solution of surfactant mixture was used for TGA. In all the TGA experiments, the sample temperature was raised from 30 to 110 °C at a rate of 20 °C/min and was kept at 110 °C for 30 min to dry the sample. The temperature was then raised at a rate of 7 °C/min to 900 °C. For the analysis of the gas resulting from the thermal combustion of the TGA system, an FTIR spectrometer equipped with a gaseous cell was used.

TEM Experiments. A portion of the NR solution was deposited on a TEM grid coated with a thin layer of SiO or carbon. Electron micrographs of NRs at room temperature were collected, then the grid was inserted into a tube furnace at a definite temperature. Each sample was heated for 10 min. The grid was transferred to the electron microscope, and the same exact location of the grid was imaged again. The heating and imaging processes were repeated for 200, 250, 270, and 330 °C. The temperature increment in all the experiments was 7 °C/min. All the images were taken using JEOL 100C and field emission Hitachi 2000 microscopes.

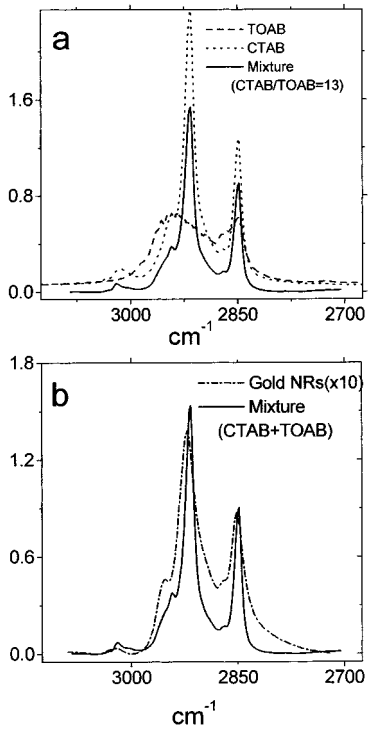

Figure 1. Stretching modes of CH_2 and CH_3 of the methylene chain for (a) a surfactant mixture and its two components and (b) FTIR spectra of gold NRs (dash−dotted line) and surfactant mixture (solid line) at the high-frequency region.

Chart 1. Molecular Structure of CTAB and TOAB

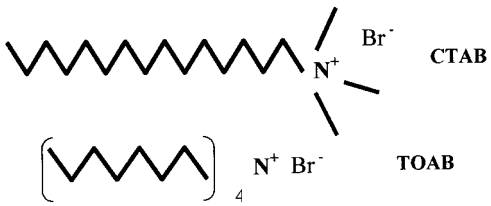

Results

FTIR Results at Room Temperature. Figure 1a represents the region 2700−3100 cm^{-1} for the surfactant mixture and its two pure components, i.e., CTAB and TOAB (Chart 1 shows the structure of these compounds). The FTIR spectra of CTAB and the surfactant mixture are very similar, and the contribution of TOAB (cosurfactant) was found to be negligible. For surfactant (Figure 1a) mixture upon binding to gold NR, the C−H symmetric

(21) Grabar, K. C.; Freeman, R. G.; Hommer, M. B.; Natan, M. J. *Anal. Chem.* **1995**, *67*, 735.
(22) He, L.; Musick, M. D.; Nicewarner, S. R.; Salinas, F. G.; Benkovic, S. J.; Natan, M. J.; Keating, C. D. *J. Am. Chem. Soc.* **2000**, *122*, 9071.
(23) Mohamed, M. B.; Ismail, K. Z.; Link, S.; El-Sayed. M. A. *J. Phys. Chem. B* **1998**, *102*, 9370.
(24) Nikoobakht, B.; Wang, Z. L.; El-Sayed. M. A. *J. Phys. Chem. B* **2000**, *104*, 8635.

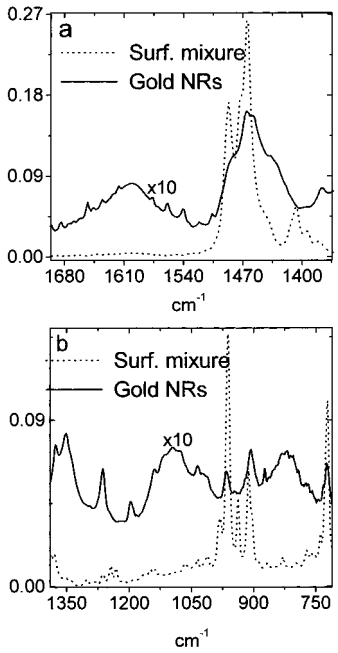

Figure 2. FTIR spectra of surfactant mixture and surfactant capped gold NRs: (a) The 1400−1680 cm^{-1} region. After the surfactant is bound to the gold surface, the CH_2 bending vibrations shift to the right and a new shoulder appears at 1430 cm^{-1}. The band at 1602 cm^{-1} is the O−H bending mode of water around the bound headgroups. (b) The 750−1350 cm^{-1} region. The formation of new peaks implies binding of the surfactant to the gold surface.

(ν_{sym}(C−H)) and asymmetric (ν_{asym}(C−H)) stretching vibrations at 2850 and 2920 cm^{-1} slightly shift to higher frequencies and the width of these bands increase as well. The peak at 2943 cm^{-1} in the surfactant mixture shifts to 2953 cm^{-1} in the gold NRs. This peak has contributions from ν_{asym}(C−H) of the CH_3 terminal group of the methylene chain[25] and ν_{sym}(C−H) of CH_3-N^+.[26]

In the surfactant mixture (Figure 2a, dashed line), the peaks (doublet) at 1473 and 1465 cm^{-1} are attributed to the CH_2 scissoring mode and account for a parallel packing of the trans methylene chains (in orthorhombic unit cell).[27−29] For gold NRs these peaks shift by about 8 cm^{-1} to lower frequency and their widths increase (Figure 2a, solid line). In this figure the shoulders at 1483 and 1430 cm^{-1} are assigned to the δ_{asym}(C−H) and δ_{sym}(C−H) of CH_3-N^+ moiety, respectively. (The reason for this assignment is discussed later.) The peak observed at about 720 cm^{-1} for both surfactant mixture and gold NRs is assigned to the rocking mode of the methylene chain.[28,29]

Figure 2b shows that for gold NRs, the intensity of $C-N^+$ stretching bands at 962, 937, and 912 cm^{-1} [30] decrease and new bands at 827, 1018, 1104, 1196, 1260, and 1350 cm^{-1} are formed. In the next section, the changes of the new bands and other peaks vs temperature are studied.

Effect of Heat on the Infrared Spectra. For the gold NR sample, by increasing the temperature from 23 to 101 °C, no significant changes appear in the region 700−1400 cm^{-1}(not shown). However, in the region 1400−1700 cm^{-1} (Figure 3) increasing the temperature, decreases the intensity of the O−H bending mode at 1601 cm^{-1}. Simultaneously the intensities of the shoulders at 1430 and 1483 cm^{-1} increase and become resolved peaks at 101 °C. The increase in the intensity of these peaks could be a result of water loss around the headgroup.

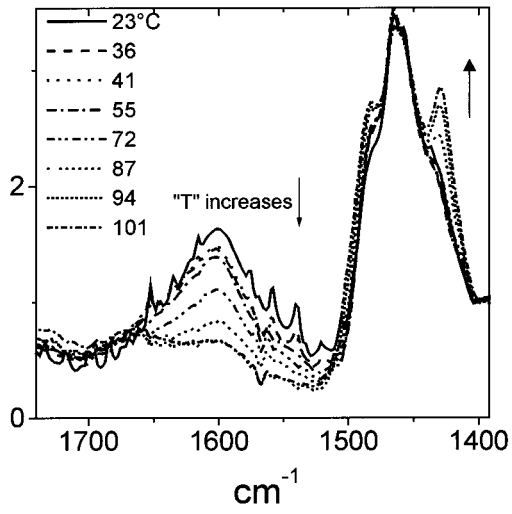

Figure 3. The effect of temperature (23−101 °C) on the surfactant capped NRs, the decay of O−H bending mode and rise of new bands related to the C−H bending modes of CH_3-N^+ are apparent.

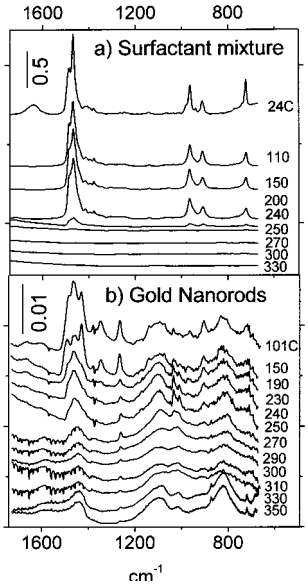

Figure 4. Effect of temperature (101−350 °C) on the FTIR spectrum of (a) surfactant mixture and (b) the gold NRs. In part a, the intensity of the $C-N^+$ stretching modes at 906 and 963 cm^{-1}, for instance, reaches zero above 250 °C. In part b, the peaks assigned to bound $C-N^+$ are more stable toward high temperature relative to the unbound headgroups.

Figure 4a illustrates the effect of changing temperature from 101 to 350 °C on the surfactant mixture spectrum. The intensity of all the peaks decreases at 250 °C. For gold NRs in Figure 4b, by increasing the temperature, the intensity of the peaks at 906, 939, and 965 cm^{-1} starts to decline, which is an indication of the gradual removal of the unbound surfactant. The broad peaks at 827, 1018, and 1104 cm^{-1} show decrease in intensity up to 300 °C, but subsequently their intensities increase such that they become comparable to the original peaks at 23 °C (see Figures 4b and 5b). This recovery in the intensities is not

(25) MacPhail, R. A.; Snyder, R. G.; Strauss, H. L. *J. Am. Chem. Soc.* **1980**, *102* (11), 3976.
(26) Umemura, J.; Kawai, T.; Takenaka, T. *Mol. Cryst. Liq. Cryst.* **1984**, *112*, 293.
(27) Umemura, J.; Cameron, D. G.; Mantsch, H. H. *Biochim. Biophys. Acta* **1980**, *602*, 32.
(28) Casal, H., L.; Mantsch, H., H.; Cameron, D., G.; Snyder, R. G. *J. Chem. Phys.* **1982**, *77* (6), 2825.
(29) Chapman, D. *J. Chem. Soc.* **1957**, *1957*, 4489.
(30) Hummel, D. O. *Analysis of surfactants*; Hanser/Gardner Publications, Inc.: New York, 1996.

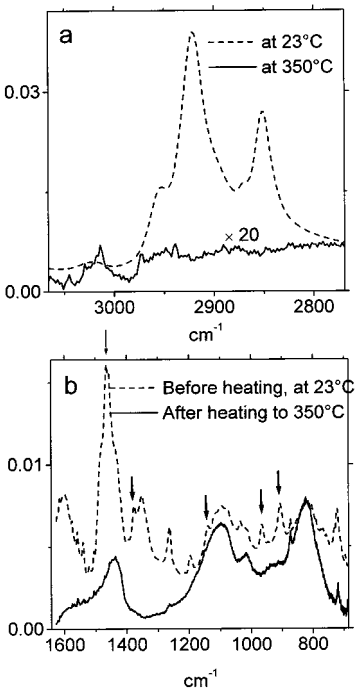

Figure 5. FTIR spectra of gold NRs at 23 and 350 °C collected at room temperature. (a) Represents the C−H stretching region. The peaks at 2960 and 3010 cm^{-1} are most likely the ν_{asym} and ν_{sym} C−H modes in CH_3-N^+ of the residual headgroups at 350 °C. (b) This figure shows the lower frequency region. In the spectrum at 23 °C, the arrows show the unbound headgroups, which desorb from the surface and are absent at 350 °C. The peaks at 820, 1018, and 1104 cm^{-1} remain stable and most likely are related to the $C-N^+$ stretching modes of the bound headgroup. The strong intensity of these peaks (at 350 °C) as compared to the peak intensities in part a shows that the organic tail is more vulnerable toward heat relative to the headgroups.

observed for ν(C−H) stretching modes at the high-frequency region (Figure 5a). Peaks at 827, 1018, and 1104 cm^{-1} due to their stability are probably the stretching modes of the bound $C-N^+$ to the gold surface. Different $C-N^+$ stretching modes in CTAB and TOAB could be a reason for the observed multiplicity of stretching modes.[30] These stable bands cannot be a result of binding of the surfactant tail via their CH_3 or CH_2 groups to the gold surface. The fact that we did not observe the characteristic [C−H···metal] vibrations,[31] strongly suggests the absence of C−H binding to the metal surface.

With an increase of temperature, the intensity of the CH_2 stretching modes in the 2800−3000 cm^{-1} region decreases for both the surfactant mixture and gold NRs, which is due to the loss of the methylene groups (see Figure 5a). Figure 5a also shows the weak peaks at about 2960 and 3010 cm^{-1} at 350 °C, which are close in frequency to the stretching modes of the CH_3-N^+ in the headgroup.

Thermogravimetric Analysis (TGA). TGA was used to further investigate the structure of the capping material on the surface of NRs. The bottom part of Figure 6 shows the TGA plot of the free surfactant and gold NRs with two different aspect ratios (curves a, b, and c, respectively) and the top part of the graph shows their derivatives.

At the bottom of Figure 6, for the surfactant mixture, the major weight loss range is from 225 to 300 °C with a weight loss peak at 297 °C. The weight loss range for gold NRs is different and spans from 150 to 600 °C. To identify the released gas from the sample, the output gas of the

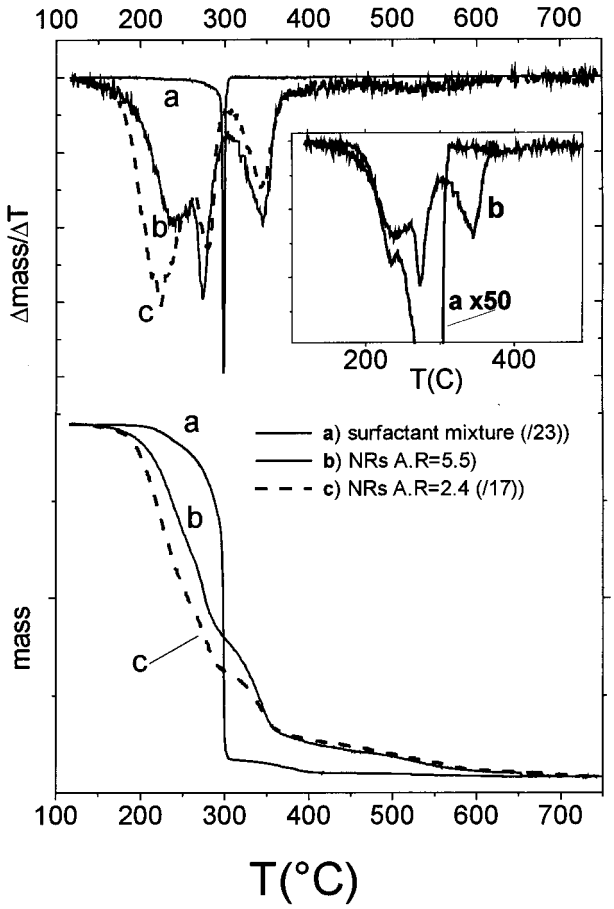

Figure 6. TGA plots and their derivatives are shown in the bottom and top part of the graph, respectively. (a) For a surfactant mixture (curve a, top part), the sharp peak at 298 °C is attributed to the surfactant molecules in aggregated form. The inset shows a closer look at curve a and that the weak weight loss peak related to the surfactant molecules in monomer form is at 235 °C. (b and c) For gold NRs with different aspect ratios (top part), the first peak is assigned to the free surfactant desorption. The second and the third peaks are attributed to the outer and inner layers desorption, respectively. It can be seen that the weight loss temperature for the free surfactant in monomer form is similar in both gold NRs and surfactant mixture.

TGA system was transferred to an FTIR with a gaseous cell. Results showed release of CO_2 at each weight loss stage. In the following part the discussion is mainly about the derivatives of the TGA plots. For surfactant mixture, only a sharp weight loss peak is observed (Figure 6, curve a). However, by closer look at this curve in the inset of Figure 6, it can be seen that in fact the surfactant mixture has two weight loss peaks. The first one starting at 190 has a maximum about 235 °C and is attributed to desorption of the surfactant molecules in monomer form, and the second peak at 298 °C is related to the surfactant molecules in the aggregated form (all the thermodynamically stable assemblies). Note that at the used surfactant concentration (0.08 M) the fraction of the surfactant molecules in monomer form is very small.

For gold NRs, two bands appear below 297 °C (relative to the surfactant mixture). These account for the presence of two types of weakly bound surfactants but with different affinities as compared to the surfactant mixture. Above 297 °C, a third peak appears, which represents the third type of surfactants with stronger affinity toward NRs. The first band (at 230 °C) is assigned to the free and/or suspended surfactants in the NR solution. One reason for

(31) Manner, W. L.; Bishop, A. R.; Girolami, G. S.; Nuzzo, R. G. *J. Phys. Chem. B* **1998**, *102* (44), 8817.

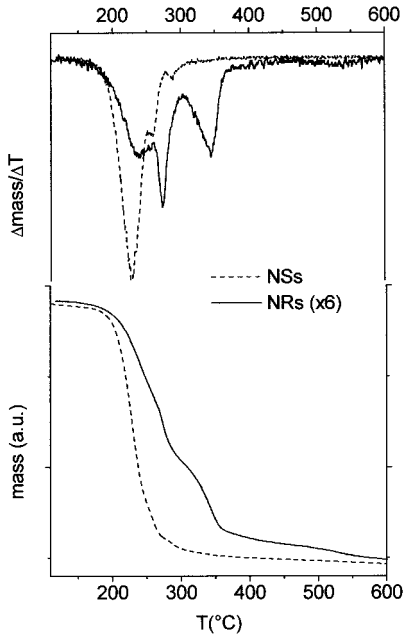

Figure 7. TGA plots for gold NSs (a) and gold NRs (b). In gold NSs the presence of weaker peaks at lower temperature shows the weaker binding of the surfactant to the gold surfaces in NSs. This could be related to the presence of a {110} facet in NRs and stronger binding of the surfactant to this facet.

Chart 2. Possible Form of the Free Surfactant Moieties (a) in the Gold NR Solution and (b) after Sample Dries (in the TGA Process)

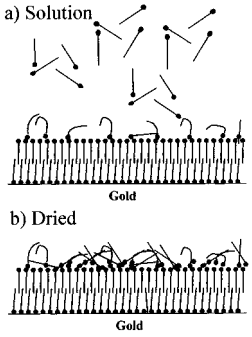

this assignment is that by further removal of the surfactant from the NR solution the intensity of the first band decreases (curves 6b,c and their derivatives illustrate this effect). In addition, this weight loss peak is very close to the weak weight loss peak observed in the surfactant mixture at 230 °C. It is assumed that in the TGA process by drying the sample upon heating, these surfactant monomers precipitate down and stick weakly to the surfactant capped gold NRs (see Chart 2). The second and the third bands at 275 and 345 °C are assigned to the unbound and bound surfactant headgroups, which form a bilayer on the gold surface. Above 400 °C, the sample loses the small amount of residual surfactant, and after 600 °C, the sample mass remains constant.

For gold nanospheres, TGA plot and its derivative are compared with gold NRs and are shown in Figure 7. For NSs (Figure 7a), a main mass loss at 230 °C and two small losses at 255 and 288 °C are apparent. In comparison with the gold NRs, the first weight loss has a similar location as compared with the first peak in NRs. The second and third peaks appear at lower temperatures, with much reduced intensities compared to the corresponding peaks in the NRs. The intensity of the first peak decreases by removing the free surfactant in the solution; however this peak cannot be removed by consecutive centrifugation because removing all the free surfactant from the solution results in the aggregation of the nanparticles. It was found that gold NSs are more sensitive to the washing process, which probably is a result of weaker capping by surfactant, and therefore a more vulnerable structure.

Discussion

The surfactant mixture includes surfactant CTAB with a long tail comprised of 16 carbon atoms and a cosurfactant with four shorter tails each made of eight carbon atoms (Chart 1). It is well-known that depending on the geometrical shape of the surfactant, the final morphology of the surfactant assembly can change.[32] Surfactant assemblies around NRs could be in two possible forms, a micellar or a bilayer structure. In fact, in the case of pure CTAB, the formation of cylindrical micelles is confirmed[33] and is also suggested for its mixture with TOAB.[34] In the micellar structure, a layer of surfactant surrounds the gold NR, where the polar side is positioned toward water. In the bilayer structure, two inner and outer layers of surfactants are present. Presumably the inner layer is bound to the gold surface via the headgroups and is connected to the outer layer through hydrophobic interactions, while the headgroups of the outer layer are in the aqueous medium (Chart 2).[32]

In this section, we attempt to evaluate each form in terms of the observed experimental data. If indeed we have a bilayer structure, the TGA data in Figure 6b or Figure 6c suggest that the second weight loss band at 273 °C can be attributed to the release of the outer layer of the bilayer. The earlier release of the outer layer compared to the surfactant mixture (at 297 °C) could be explained by the fact that only hydrophobic interactions are present between the two layers around NR. According to the FTIR data in Figure 5b, the peaks from the outer layer disappear above 273 °C. Finally the third band at 344 °C (Figure 6b) is assigned to the release of the inner layer, which experiences stronger binding of the headgroup to the gold surface.

In Figure 3, for gold NRs, the O−H bending mode at 1602 cm^{-1} (which unusually shifted to lower frequency) and the O−H stretching modes at 3340 and 3450 cm^{-1} (not shown) show that water molecules around the headgroups are possibly in a restricted state (at 23 °C).[35] These water molecules could H-bond to the bromide ion of the headgroup or H-bond to each other.[36] With increase of the temperature, the water content decreases. At the same time the intensity of the peaks at 1430 and 1483 cm^{-1} increases (see Figure 3). Figure 8a illustrates the change in the water content around the bound headgroups by increasing the temperature. Figure 8b shows the peak intensities for peaks located at the region 1260−1483 cm^{-1} of the FTIR spectrum of gold NRs. The intensities of these peaks reach a maximum at 100−150 °C, which coincides with the loss of water around the surfactant headgroups (note that there is no organic loss at this temperature). The headgroup vibrations (e.g., peaks at 1430 and 1480 cm^{-1}) due to their close proximity to the water molecules

(32) Israelachvili, J. N. *Intermolecular and Surface Forces*, 2nd ed.; Academic Press: New York, 1985.
(33) Tornblom, M.; Henriksson, U. *J. Phys. Chem. B* **1997**, *101* (31), 6030.
(34) Chang, S. S.; Shih, C. W.; Chen, C. D.; Lai, W. C.; Wang, C. R. C. *Langmuir* **1999**, *15*, 701.
(35) Gray, G. W., Winsor, P. A., Eds. *Liquid Crystal and Plastic Crystals*; Ellis Horwood: Chichester, 1974; Vol. 1, p 199.
(36) Kawai, T.; Umemura, J.; Takenaka, Kodama, M.; Ogawa, Y.; Seki, S. *Langmuir* **1986**, *2*, 739.

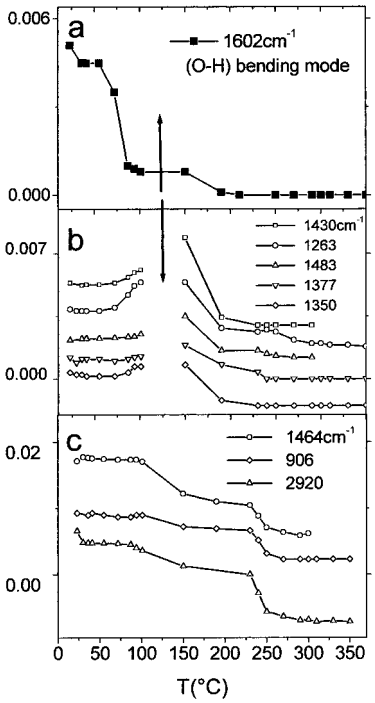

Figure 8. For FTIR of gold NRs, The peak intensities in the region 800−1600 cm^{-1} (see Figure 5b) are plotted against temperature for gold NRs. (a) Shows change in the intensity of the O−H bending mode upon heating. (b) Represents the peaks that change by decreasing the amount of water around the headgroup. (c) Shows the peaks that have a major change in their intensities at 250 °C, because of the release of the unbound surfactant at this temperature.

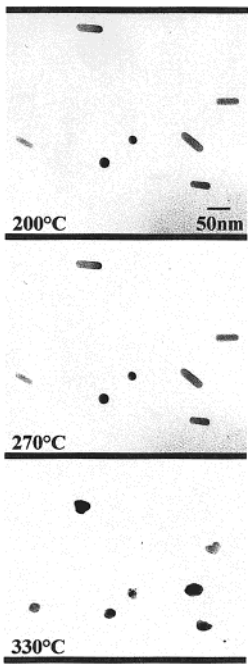

Figure 9. Electron micrographs of gold NRs at different temperatures. A similar spot on the TEM grid was inspected at each temperature. The shape transformation at 330 °C coincides with the third weight loss peak in TGA, where the surface coverage starts to decline (Figure 6b or Figure 6c). Note that the spotted NR solution contains a few percent of gold NSs as well.

on the surface are expected to be more sensitive toward water loss as compared to the methylene scissoring mode (1465 cm^{-1}). The vibrations shown in Figure 8b were attributed to the bending modes of the headgroup ($-CH_2-(CH_3)_3N^+Br^-$). These vibrations all show a similar pattern in intensity change. The change in the intensity of these peaks could be due to the H-bond breakage between the water and bromide ion and among the water molecules around the headgroups or rearrangement of the headgroups relative to the gold surface.

In the region 800−1600 cm^{-1} (Figure 8c), another class of peaks was found in which a major intensity loss occurs about 250 °C. This is attributed to the contribution of the unbound surfactants in these peaks, which desorbs from the surface. The result of TGA (Figure 6b or Figure 6c) is in agreement with the above observation.

The relative stability of the peaks at 820, 1028, and 1105 cm^{-1} at 350 °C is an indication of strong affinity of the corresponding bonds to the gold surface. These peaks were assigned to the stretching modes of the bound $C-N^+$ to the gold surface (which are shifted relative to their unbound stretching vibrations, i.e., 906−936 cm^{-1} region). In Figure 1b, for the surfactant mixture the peak at 2942 cm^{-1} shifts to 2955 cm^{-1} (in gold NRs), which is additional evidence for the proximity of the headgroup to the gold surface. The intensities of the C−H vibrations in the region 2800−3000 cm^{-1} are negligible at 350 °C; however peaks at 820, 1028, and 1100 cm^{-1} are still strong. This could suggest that while most of the methylene chains are desorbed at 350 °C, still a large fraction of the headgroups are present on the gold surface. Overall bending and stretching modes of C−H and $C-N^+$ bonds show binding of the headgroup to the gold surface.

In an electrophoresis experiment, we found that NRs tend to go toward the negative electrode, which infers that net positive charges are on their outer layer. In our TEM experiments, Figure 9, we found that in the first and second weight loss peaks, i.e., temperature region 190−270 °C, the NR length decreases by less than 10% as compared to the length of NRs at 25 °C. However, the major change takes place in the 300−330 °C temperature region. This temperature range is near the third peak, where the inner layer begins to desorb or decompose. This indicates that the inner layer has the major role in stabilizing the shape of the NR. Considering the micellar model, only one layer of the surfactant is around the NRs and therefore at most two weight loss peaks are expected to be observed in TGA. The first weight loss corresponds to the loss of the suspended surfactants in the solution. The second weight loss peak corresponds to the micellar layer on the surface. According to this model, the third weight loss peak remains unassigned. In addition, the presence of a layer of surfactants in which the polar head is toward the solution dictates the presence of C−H−metal bonds. However, FTIR data do not support this type of surfactant binding. The observed results agree better with a surfactant bilayer structure around gold NRs.

The CH_2 stretching and scissoring modes have been used to extract information about the nature of the surfactant packing on the gold surface. Table 1 compares the CH_2 stretching vibration frequencies for CTAB in the monomeric state, in micellar form, in a mixture with TOAB, and on capped gold NRs. As seen, the CH_2 vibration frequencies in the gold NRs are lower than that in the micellar form and higher than the surfactant mixture.[37] This energy shift has been interpreted in terms of the structural order of methylene chains.[37] In Figure 1b, for surfactant mixture, the lower frequency and narrower

(37) Weers, J. G.; Scheuing, D. R. Micellar shape to rod transitions. In *Transform Infrared Spectroscopy in Colloid and Interface Science*; ACS Symposium Series 447; American Chemical Society; Washington, DC, 1991.

Table 1. Stretching Modes of C−H in (CH_2) for Surfactant CTAB in Its Monomeric Form, Micellar Form, Packed Form on the Surface of Gold NRs, and Mixed with TOAB

state	monomer (HTAB)[19]	micelle (HTAB)[19]	surfactant capped NRs	surfactant mixture dried from solution (CTAB & TOAB)
CH_2 stretching vibrations, cm^{-1}	2930, 2860	2923, 2853	2921, 2851	2917, 2849

bandwidths account for methylene chains with more ordered structure. For gold NRs, larger bandwidths and higher frequencies are believed to be due to an increase in the number of gauche conformers in these chains.[19,37,38]

The amount of shift in the vibrational frequencies of stretching and bending modes of CH_2 is found to depend on the surfactant surface coverage. For particles with high surface coverage, there is a smaller shift in comparison with particles having low surface coverage.[19] The above facts in conjunction with the results in Figure 1 and Table 1 suggest a high surfactant coverage on the gold NR surface. It also suggests the fraction of gauche conformers in the gold NRs is increased compared to the surfactant mixture, which most likely is a result of the presence of the cosurfactant in the bilayer.

The CH_2 scissoring (bending) modes can also be used to acquire information about chain packing and chain rotation. However, in this study due to their overlap with CH_3 bending modes[28] the rocking mode of the methylene chain was used instead. For both surfactant mixture and gold NRs, the presence of the singlet peak at about 720 cm^{-1} shows that the methylene chains have free rotation in their hexagonal packed structure. This peak for the surfactant mixture in solid form (mixed with KBr) is a doublet (not shown), which accounts for an orthorhombic unit cell for the packed surfactants.[28,29] The absence of the doublet peaks at 719 and 730 cm^{-1} rules out the possibility of having a crystalline structure for the organic core of the bilayer around gold NRs.

As shown in Figure 7 and discussed in the previous sections, the nanorods and nanospheres both have three weight loss peaks, one due to the extra surfactant (the low-temperature peak) and the other two peaks because of the bilayer structure around the nanoparticles. In explaining the differences in the TGA plots of NRs and NSs, one might attribute the appearance of the second and third weight loss peaks at higher temperatures in NRs to the presence of {110} facet to which binding of the surfactant is expected to be stronger than binding to {111} or {100} facets.[39] The higher intensity of the weight loss peaks shows larger release of surfactant and could be reflection of a well-defined bilayer structure around NRs. The observed shift in the second weight loss peak (273 °C) relative to the surfactant mixture (298 °C) could be due to a weaker hydrophobic effect present in the bilayer around gold NRs. It is important to know that NRs possess three types of facets, i.e., {100}, {110}, and {111},[40] while gold NSs do not have the {110} facet. This facet also has a higher surface energy as compared to the others and therefore greater tendency to bind to surfactant. For NSs, the weaker intensities of the second and third peaks reflect a lower amount of desorbed surfactant. This could lead to the conclusion that NSs do not have a well-defined bilayer structure as compared to NRs. As a side effect, the hydrophobic interaction between the inner and outer layer would be weaker, which is consistent with the lower temperatures for the second and third peaks in NSs.

Conclusions

Our results suggest that the two cationic surfactants, i.e., CTAB as the major and cosurfactant TOAB as the minor component in the mixture, form a bilayer structure around gold NRs rather than a micellar form. Water molecules are present in the vicinity of the gold surface and most likely are H-bonded together and to the bromide counterions. Effect of temperature on water molecules was used to assign the peaks associated with vibration modes of the headgroup. Methylene vibration frequencies indicate that these chains are packed parallel, but the free rotation and the number of gauche conformers in the chains are increased in the surfactant-capped NRs. A decrease in the number of trans chains is probably because of the presence of the cosurfactant. FTIR and TGA support the bilayer structure, and TEM results are in agreement with these conclusions. The major shape transformation in NRs occurs at 300−330 °C (ambient atmosphere), where the inner layer gradually desorbs from the surface. Finally TGA results suggest that surfactants bind to NRs stronger than to the NSs. The results suggest that surfactants around NRs form a more defined bilayer structure relative to NSs. This was attributed to the presence of the {110} facet in the NRs, to which the surfactant binds stronger.

Acknowledgment. This research was supported by NSF CHE-9727633.

LA010530O

(38) Naselli, C.; Rabolt, J. F.; Swalen, J. D. *J. Chem. Phys.* **1985**, *82*, 2136.

(39) Wang. Z. L.; Gao, R. P.; Nikoobakht, B.; El-Sayed, M. A. *J. Phys. Chem. B* **2000**, *104* (23), 5417.

(40) Wang, Z. L.; Mohammed, M. B.; Link, S.; El-Sayed, M. A. *Surf. Sci.* **1999**, *440*, L809.